HHS Public Access

Author manuscript

Neuroscience. Author manuscript; available in PMC 2021 September 01.

Published in final edited form as:

Neuroscience. 2020 September 01; 443: 44–58. doi:10.1016/j.neuroscience.2020.06.036.

Lateralized Connectivity between Globus Pallidus and Motor Cortex is Associated with Freezing of Gait in Parkinson's Disease

Óscar Miranda-Domínguez[a], **Anjanibhargavi Ragothaman**[b], **Robert Hermosillo**[a], **Eric Feczko**[a,c], **Rosie Morris**[d], **Patricia Carlson-Kuhta**[d], **John G. Nutt**[d], **Martina Mancini**[b,d], **Damien Fair**[a,e,f], **Fay Horak**[a,b,d,*]

[a]Department of Behavioral Neuroscience, Oregon Health & Science University, 3181 SW Sam Jackson Park Road, Portland, OR 97239, United States

[b]Department of Biomedical Engineering, Oregon Health & Science University, 3181 SW Sam Jackson Park Road, Portland, OR 97239, United States

[c]Department of Medical Informatics and Clinical Epidemiology, Oregon Health & Science University, 3181 SW Sam Jackson Park Road, Portland, OR 97239, United States

[d]Department of Neurology, Oregon Health & Science University, 3181 SW Sam Jackson Park Road, Portland, OR 97239, United States

[e]Department of Psychiatry, Oregon Health & Science University, 3181 SW Sam Jackson Park Road, Portland, OR 97239, United States

[f]Advanced Imaging Research Center, Oregon Health & Science University, 3181 SW Sam Jackson Park Road, Portland, OR 97239, United States

Abstract

Freezing of gait (FoG) is a brief, episodic absence or marked reduction of forward progression of the feet, despite the intention to walk, that is common in people with Parkinson's disease (PD). We hypothesized that not only motor, but higher level cognitive and attention areas may be impaired in freezers. In this study, we aimed to characterize differences in cortical and subcortical functional connectivity specific to FoG. We examined resting state neuroimaging and objective measures of FoG severity and gait from 103 individuals (28 PD + FoG, 36 PD - FoG and 39 healthy controls). Inertial sensors were used to quantify freezing severity and gait. Groups with and without FoG were matched on age, disease severity, cognitive status, and levodopa medication. MRI data was processed using surface-based registration. High-quality imaging data were used to characterize differences in connectivity specific to FoG using a pre-defined set of Regions of Interest (ROIs) and validated using whole-brain connectivity analysis. Associations between functional

*Correspondence to: Fay Horak, Department of Neurology, Oregon Health & Science University, OP-32, Portland, OR 97239, United States. horakf@ohsu.edu (F. Horak).

APPENDIX A. SUPPLEMENTARY DATA

Supplementary data to this article can be found online at https://doi.org/10.1016/j.neuroscience.2020.06.036.

COMPETING INTERESTS

FH has a significant financial interest in APDM, a wearable sensors company that may have a commercial interest in the results of this research and technology. This potential conflict has been reviewed and managed by OHSU.

connectivity and objective measures of FoG were determined via predictive modeling using hold-out cross validation. We found that connectivity between the left globus pallidus (GP) and left somatosensory cortex and between two brain areas in the default and insular/ vestibular networks exhibited significant differences specific to FoG and were also strong and significant predictors of FoG severity. Our findings suggest that the interplay among motor, default and vestibular areas of the left cortex are critical in the pathology of FoG.

Keywords

freezing of gait; functional connectivity; globus pallidus; attention systems; Parkinson's disease

INTRODUCTION

Freezing of gait (FoG), the brief, episodic absence or marked reduction of forward progression of the feet despite the intention to walk (Nutt et al., 2011), is a disabling disorder of unknown etiology, with FoG events most often occurring during gait initiation or turning. FoG is common in people with Parkinson's disease (PD) and can be triggered by various factors, such as physical barriers, performing an additional task when walking, and anxiety (Kasper, 2015). This variety of contextual triggering factors suggests that not only motor, but cognitive and limbic networks may be impaired in FoG (Shine et al., 2013b). FoG imposes a significant burden on patients since, besides its dramatic negative impact on mobility, FoG often leads to imbalance and falls (Nonnekes et al., 2015; Snijders et al., 2016; Okuma et al., 2018).

FoG is often hard to measure (or even observe) clinically and in the laboratory (Nonnekes et al., 2015; van Dijsseldonk et al., 2018; Mancini et al., 2019). In research or clinical practice, FoG is often assessed by a freezing of gait questionnaire (NFOG-Q) designed to identify people who experience FoG in the past month (yes or no) and to gauge severity by frequency and impact on daily life (Nieuwboer et al., 2009). More recently, body worn sensors placed on the lower limbs have been used to identify gait features that are consistently associated with FOG (Moore et al., 2009, 2011; Mancini et al., 2019), such as trembling of the knees (Okuma, 2006; Moore et al., 2008) and shuffling of the feet (Jankovic, 2008).

Previous studies characterizing brain surrogates of FoG have not resulted in consensus. Several groups have used neuroimaging aiming to characterize altered patterns of functional connectivity specific to FoG. Functional connectivity provides an indication of which functional neural networks work together with correlated, or anticorrelated activity, even at rest (Biswal et al., 1995; Fox and Raichle, 2007; Holodny, 2009; Grayson and Fair, 2017; Miranda-Dominguez et al., 2018). Using this approach, our group found asymmetrical functional (and structural) connectivity between the PPN and the supplementary motor area (SMA) in people with PD and FoG (Fling et al., 2013, 2014). Other groups have also shown that multiple non-motor networks including the visual, default, frontoparietal, attention and opercular networks are altered in FoG (Tessitore et al., 2012; Shine et al., 2013a; Canu et al., 2015; Fasano et al., 2015; Lenka et al., 2016; Gilat et al., 2018; Maidan et al., 2019). Case-reports of FoG in people without PD have found that lesions to several brain structures,

including the globus pallidus (GP) (Fève et al., 1993; Merello et al., 2001; Krystkowiak et al., 2006), pedunculopontine nuclei (PPN) (Kuo et al., 2008), dorsomedial cerebellum (Fasano et al., 2017), among others, lead to the development of FoG.

The abundance of disparate findings underscores the necessity for standardized neuroimaging methodologies. Standardization of methods to process neuroimaging data using stringent quality assessments (Glasser et al., 2013; Mills et al., 2018; Miranda-Dominguez et al., 2018; DCAN-Labs, 2019) as well as reproducible delineation of Regions of Interest (ROIs) and functional systems (Gordon et al., 2014), together with objective measures of FoG (Mancini et al., 2018, 2019), and matching groups based on disease severity might lead to more parsimonious and generalizable findings about the brain areas related to FoG. In this study, we hypothesize that FoG is associated with differences in functional connectivity between subcortical and cortical brain areas, including non-motor cortical areas. To test this hypothesis, we conducted various analyses at different spatial resolutions (whole-brain as well as ROI seed-based analyses) in order to establish and ascertain that the identified differences in functional connectivity are a prominent feature in FOG.

EXPERIMENTAL PROCEDURES

Participants

A total of 111 participants were enrolled in the study. Eight participants did not have MRI data of enough quality (extremely high head movement leading to unclear definition of gray and white matter and unreliable BOLD data), ending up with a sample 103 participants of which 39 were healthy controls (Ct), 28 PD + FoG, and 36 PD − FoG. PD + FoG and PD − FoG had idiopathic PD clinically diagnosed by a movement disorders specialist using UK Brain Bank Criteria (Gibb and Lees, 1989). From those, we selected a subsample of highest data quality (i.e.; most stringent head movement threshold of 0.3 mm whole brain framewise displacement, (see motion censoring below)) for resting state data to characterize differences in functional connectivity specific to freezing. In an effort to match people with and without FoG for disease severity, we matched the remaining participants for age, MDS-UPDRS-III (Goetz et al., 2008), MoCA (Nasreddine et al., 2005), and LED medication (Tomlinson et al., 2010), ending up with a sample size of 43 that contains 16 Ct, 13 PD + FoG and 14 PD − FoG. Reliability of findings and correlations between functional connectivity with FoG measures were then assessed using the larger group of lower quality data (i.e.; less stringent head movement threshold of 0.5 mm and not matched for severity of disease). Sample count and group's scores are reported in Table 1.

All tests were conducted in the practical 'Off' levodopa state, after withholding anti-parkinsonian medication for ≥12 h. Inclusion criteria for subjects with PD were: (1) between 50 and 90 years old, (2) no major musculoskeletal or peripheral disorders (other than PD) that could significantly affect their balance and gait, and (3) ability to stand and walk unassisted for 20 feet. Healthy, elderly adults within the same age range were recruited from the community. Exclusion criteria for both groups were any other neurological disorders or musculoskeletal impairments that interfere with gait or balance, claustrophobia, and inability

to follow instructions. Severe tremor was another exclusion criteria to ensure good quality MRI.

Participants were included in the PD + FoG group if: (1) they answered 'yes' to the first question of the NFOG-Q (Nieuwboer et al., 2009): "Have you experienced FoG in the past month?" after reviewing the video, OR (2) FoG was observed in the laboratory during testing.

All subjects gave written informed consent in accordance with the Declaration of Helsinki. The protocol was approved by the Oregon Health & Science University, OHSU (#4131) and the OHSU/VAPORHCS joint IRB (#8979). These participants were part of a larger interventional study (Clinical Trials NCT02231073 and NCT02236286), of which we used the baseline session of the study.

Procedure

Participants underwent two mornings of testing with Day-1 including neuroimaging (see below), and Day-2 including instrumented assessment of mobility in the laboratory, or vice versa. Subjects with PD were clinically rated by a trained examiner on the Motor Section (III) of the Movement Disorders Society Unified Parkinson's Disease Rating Scale (MDS-UPDRS) (Goetz et al., 2008). Global cognition was measured with the Montreal Cognitive Assessment (MoCA (Nasreddine et al., 2005)), and levodopa equivalent daily dosage (LEDD) was calculated (Tomlinson et al., 2010).

Mobility data collection and processing

Each participant was outfitted with 8 inertial sensors (APDM, Inc., Portland, OR, USA), worn on the sternum, lumbar spine, bilaterally on the wrists, shins, and feet. Each inertial sensor recorded tri-axial accelerations, angular velocities, and magnetic field at 128 Hz. However, only the FoG ratio and the Pitch angle at heel strike led to significant differences for each paired comparison (Ct and PD + FoG, Ct and PD − FoG, PD + FoG and PD − FoG) using our sample matched on age, disease severity, cognitive status, and levodopa medication, as shown in Table S1. Hence, we only used FoG ratio and the Mean Foot Strike Angle to characterize associations between functional connectivity and objective metrics of FoG. Those two motor tasks were measured as follows: (1) FoG task – 1-min-long turning, in which participants made 360° turns on the spot, alternating between clockwise and anti-clockwise turns as fast as they could safely perform, and (2) Gait task – a self-paced, 2-minute walking trial, in which participants walked back and forth continuously between two lines 7.62 m apart with 180 degree turns.

Outcome measures of mobility

To calculate FoG severity, raw data from the antero-posterior accelerations of the shin was analyzed during the turning in place task following a previously published methodology (Mancini et al., 2017). Briefly, the power spectral density was first calculated for the turning trial and normalized for each subject to the area under the power spectral density curve. Then, a FoG ratio was calculated as the ratio between the square of the total power in the frequency band corresponding with FoG episodes (3–8 Hz), and the total power in the

frequency band corresponding with locomotion (0.5–3 Hz) (Moore et al., 2008; Mancini et al., 2017). Higher FoG-ratio scores therefore indicate greater FoG severity (Mancini et al., 2017). In addition, Mobility Lab software V2 (APDM, Inc.) was used to calculated the pitch angle at heel strike during the portion of steady state walking for the walking trial (automatically excluding turns).

MRI data collection and processing

MRI data collection.—Imaging data was acquired using a 3 Tesla Siemens Trio scanner with a 12-channel head coil. T1-weighted (TR = 2300 ms, TE = 3.58 ms, voxel size = 1 mm x 1 mm x 1.1 mm, slices = 160) and T2- weighted (TR = 3200 ms, TE = 497 ms, voxel size = 1 mm3, slices = 160) images were acquired for co-registration. Two 10-min resting state (eyes open while viewing a standard crosshair) BOLD images were obtained using a gradient-echo planar imaging (EPI) sequence (TR = 2000 ms, TE = 30 ms, field of view = 240 mm, flip angle = 90°, voxel size = 3.75 × 3.75 × 3.8 mm). We collected 20 min of resting state data in total to maximize the number of frames (volumes) that can be preserved after motion censoring. See Supplementary Materials for additional details.

MRI data preprocessing.—Data was processed using surface-based registration following an adapted version of the workflow pipelines from the HCP (Glasser et al., 2013; Gilat et al., 2018; Miranda-Dominguez et al., 2018; DCAN-Labs, 2019) (available in github at https://github.com/DCAN-Labs/abcd-hcp-pipeline), that includes the use of FSL (Smith et al., 2004; Woolrich et al., 2009; Jenkinson et al., 2012), FreeSurfer (Dale et al., 1999; Fischl and Dale, 2000; Desikan et al., 2006), Connectome Workbench (Marcus et al., 2011) and ANTs (Avants et al., 2011). Time-courses are reported in the standard grayordinate space (Glasser et al., 2013), which contains 91,282 gray-ordinates (vertices and voxels) in the gray matter (surface and subcortical ROIs). For resting state data, after slice time correction, the BOLD data is corrected for field distortions and registered preliminary to the first frame using a 6 degrees of freedom linear registration. After this initial alignment, the average frame is calculated and used as final reference. Next, the BOLD data is registered to this final reference and to the T1- weighted volume, all in one single step, by concatenating all the individual registrations into a single transformation matrix. See Supplementary Materials for additional details.

Nuisance correction.—Additional steps consisted of regressing out the whole brain, ventricle, white matter average signals, and displacement on the six degrees of freedom's rigid body registration parameters, their derivatives and their squares. Finally, time-courses are filtered using a first order Butterworth band pass filter with cutting frequencies between 0.009 and 0.080 Hz. The filter is applied in the forward and backward direction to cancel temporal delays (Friston et al., 2000; Fair et al., 2007, 2009, 2020; Power et al., 2013).

Motion censoring.—We discard data if a participant moves beyond "acceptable" limits (0.3 mm framewise displacement (FD), see (Power et al., 2012) for calculation). Removed frames are selected based on: (1) their total relative movement in any direction/rotation or (2) their proximity to *discarded* frames (Power et al., 2013).. The removal of frames follows the criteria outlined in Power 2013 (Power et al., 2013), whereby frames that exceed the

movement threshold are excluded. Additionally, if 2 frames are that exceed the movement threshold are within 5 frames of each other, the frames between them are also excluded. Only participants with at least 5 min of head movement less than 0.3 mm (Power et al., 2012, 2013; Fair et al., 2013) were included in the analysis. Next, we kept constant the number of frames by sampling randomly 5 min of data with a frame displacement less than 0.3 mm. Hence, connectivity matrices were calculated using the same amount of unbiased data for all surviving participants.

ROIs and functional networks.—Resulting BOLD data from each gray-ordinate were parcellated using a predefined functional atlas that contains 286 ROIs grouped into 12 functional networks (Gordon et al., 2014). In this atlas, ROIs were defined by looking at the homogeneity of connectivity patterns of neighboring voxels using two independent datasets ($n1$ = 120 and $n2$ = 108). Resulting ROIs overlapped with architectonic maps. Functional networks were identified using a robust and validated clustering algorithm (community detection) (Rosvall and Bergstrom, 2008) and correspond to well-defined functional systems. The resulting functional networks (and ROI count) are: Auditory (Aud, n = 24), Cingulo Opercular (CiO, n = 40), Cingulo Parietal (CiP, n = 5), Default (Def, n = 41), Dorsal Attention (DoA, n = 32), Fronto-Parietal (FrP, n = 24), Retrosplenial Temporal (ReT, n = 8), Somato-sensory lateral (Sml, n = 38), Somato-sensory medial (SMm, n = 8), Salience (Sal, n = 4), Ventral Attention (VeA, n = 23), and Visual (Vis, n = 39), as shown in Fig. 1. In addition to these functional networks, we added the subcortical segmentations derived from FreeSurfer to define a subcortical network (Sub, n = 19 including the caudate, putamen, GP, accumbens and cerebellum (Fischl et al., 2002, 2004), hence we used 305 ROIs (286 cortical + 19 subcortical) in total in this study.

Functional connectivity.—Functional connectivity was characterized for each participant using Pearson correlations. Correlation coefficients were calculated for each ROI pair using only low head-movement frames, keeping constant the number of frames across participants. Given 305 ROIs, there are 46,360 unique connections, which were grouped per functional system pair, as shown in Fig. 1. Given 13 networks there are 92 ($13 \times (13 + 1)/2 = 91$) unique functional system pairs (Aud-Aud, Aud-Def, etc.).

Statistical analysis

The goal of the study is to characterize differences in functional connectivity between freezers and nonfreezers and between people with PD and controls and to identify associations between imaging and objective measures of FoG. Three analyses were used: (1) repeated measures ANOVA to identify ROIs with differences in functional connectivity specific to FoG; (2) whole-brain connectivity analysis based on identified ROI seeds to characterize the spatial extent of differences in functional connectivity between freezers and nonfreezers, not constrained by the delineation of ROIs and networks imposed by the functional atlas used in this study (Gordon). This step is needed to ensure the cortical areas found to be significant are truly represented in this older population and not an artifact secondary to registration problems between the atlas used to define brain areas and each participant's brain. (3) predictive modeling to characterize associations between functional

connectivity and FoG behavior. Details of each method are presented in the following subsections.

Repeated measures ANOVA to identify ROIs with differences in functional connectivity specific to FoG.—We used a repeated measures ANOVA test to identify potential differences in functional connectivity among diagnostic groups at two resolutions: individual connections and functional systems (Kovacs-Balint et al., 2019). For this analysis, neuroimaging data are reported at the resolution of ROIs and functional networks, as outlined by Gordon (Gordon et al., 2014). The ANOVA used the variable “Diagnosis” (Ct, PD + FoG, and PD − FoG) as between-factor. “Connection” and ‘functional system pair” were used as repeated variables, i.e., within-factors. *p-values* were corrected for multiple comparisons using the false discovery rate (FDR) method and epsilon-adjusted values are used if the asymmetry assumption is not met, as assessed by the Mauchly’s test. Significance threshold for significance was set to 0.05.

To identify specific functional system pairs driving differences between diagnostic groups, we ran 92 repeated measures ANOVA tests (one test for each functional system pair) and resulting *p-values* were corrected for multiple comparisons using the FDR method. To identify connections with differences between specific diagnostic groups, we ran post-hoc *t*-tests for each ROI pair where the *p-values* were corrected for multiple comparisons using FDR.

Whole-brain connectivity analysis to characterize the spatial extent of cortical areas with differences in functional connectivity specific to FoG.—To calculate differences in functional connectivity from a specific seed, we calculate the Pearson’s correlation coefficient between a seed (i.e., the left GP) and each grayordinate (n = 91,282) for each participant. Next, we performed an ANOVA test on each grayordinate using FSL PALM (Winkler et al., 2014) to identify brain areas with differences among diagnostic groups and corrected for multiple comparisons via permutations (Smith and Nichols, 2009; Winkler et al., 2014). Results of each ANOVA-test were converted to Z-scores, which were then thresholded at 1.96 to determine putative clusters. These clusters were contiguous brain regions where the Fisher $Z > 1.96$ (i.e. these represent the ~5% of correlation values). To correct for multiple comparisons, cluster sizes were then permutation-based tested with 10,000 permutations, to test where the cluster extent was significant, (a was set at -log p = 1.3) using the well-established threshold-free cluster enhancement (TFCE) method (Smith and Nichols, 2009).

To identify the grayordinates driving the differences between diagnostic groups we ran series of *t*-tests between each diagnostic group pair and corrected *p-values* for multiple comparisons. These tests were constrained to the grayordinates belonging to the cluster identified by the previous analysis and the count of comparisons corresponds to the cluster size (in grayordinates count).

Predictive modeling to characterize associations between functional connectivity and FoG behavior.—We used partial least squares regression (PLSR) models to investigate whether behavioral outcomes of FoG severity and gait were predicted

by functional connectivity. Outcome was predicted using PLSR (Rosipal et al., 2005; Rudolph et al., 2017, 2018) and goodnes of the fit is reported using out-of-sample data holding 10% of the sample for cross-validation and repeating this approach 10,000 times. Null-hypothesis data (N = 10,000) were created via permutations using the same steps. In this method, a linear model is fit such that redundancy (covariance) is minimized by calculating a new set of variables coming from the original predictor variables. The new set of variables was built as a linear combination of the original variables (Rosipal et al., 2005).

Data availability

Data and code will be made available via OHSU library website and GitHub, respectively.

RESULTS

Differences in functional connectivity among diagnostic groups

Functional connectivity was significantly different among diagnostic groups, functional system pairs, connections and their interactions (Table S2). Post-hoc analyses revealed that only nine functional system pairs (Sml and Sml, Def and SMm, SMm and Sml, Sml and Sub, SMm and Sub, CiO and Def, Def and DoA, Def and Sub, DoA and Vis) had differences among the three diagnostic groups and that only the groups Ct *versus* PD + FoG as well as Ct *versus* PD − FoG were significantly different (i.e.; Ct *versus* PD). However, functional connectivity between networks for PD + FoG were not significantly different from PD − FoG (Table S3).

Differences in functional connectivity between freezers and non-freezers

In the absence of specific differences between PD + FoG and PD − FoG across networks, we looked at differences across individual connections since the previous analysis revealed a significant effect for this interaction (p = 0.008, see Table S2). Post-hoc analyses for the interactions between Diagnosis and Connectivity revealed that three connections belonging to the motor, default and auditory/vestibular systems had significant differences in functional connectivity ($p < 0.05$, corrected, as shown in Table S4) for each group pair (Ct/PD + FoG, Ct/PD − FoG, and PD + FoG/ PD − FoG), as shown in Fig. 2. The significant differences between PD + FoG and PD − FoG were: (1) left GP-left medial sensorimotor cortex in Brodmann area 3b (Gordon ROI 59); (2) default network, (Gordon ROI 154 covering partially the Brodmann areas 46 and 8A dorsal) – left vestibular network (Gordon ROI 69 covering partially the lateral Belt area in the early auditory cortex and the retroinsular cortex), and (3) left GP-left lateral sensorimotor cortex in Brodmann areas 3a and b (Gordon ROI 38). Fig. 2 indicates the location of each ROI and Table S4 reports the corrected p-values for the post-hoc comparisons for each group pair.

For the two left GP-left motor ROI pairs, the control group had negative connectivity, whereas the PD groups had more connectivity than the Ct group, with the PD + FoG group switching from negative to positive connectivity values (Fig. 2 left and right plots). For the default-vestibular ROI pair, functional connectivity in the control group was slightly less than zero and the PD groups had significantly larger negative connectivity (Fig. 2 center).

For all three connections, connectivity values for the PD − FoG group were between the values for the Ct and PD + FoG groups.

To determine the robustness of the findings at different motion-censoring thresholds using both matched and unmatched data, we looked at the three connection pairs we found to be significant in the following subsamples (see Table 1 for further details). In all these three cases, the connection pairs including the left GP exhibited significant, or nearly significant, differences between freezers and non-freezers, as shown in Fig. S1, suggesting low likelihood our findings are a false positive.

Differences in functional connectivity from the left GP

As our analysis indicated that the left GP exhibit significant differences in functional connectivity between PD + FoG and PD − FoG and given the relevance of the GP in PD, we further investigated for differences in functional connectivity between the PD + FoG and PD − FoG groups in an exploratory way that did not constrain the analysis to predefined ROIs or networks from the Gordon set. For this analysis, instead of using a predefined set of ROIs, we calculated the correlation coefficient between the left GP and each grayordinate (n = 91,282, see Methods) for each participant. ANOVA tests on each grayordinate found that the differences between groups were constrained to the bilateral motor cortex (see Fig. 3 panel A).

Mean functional connectivity between the left GP and the identified cluster in the left motor cortex was strongly associated with freezing status (odds ratio = 71.5, CI: [5.77, 898.64], Fisher's exact test p = 6.88e-5), where PD + FoG exhibited positive mean correlations between the left GP and the identified cluster in the motor cortex (11 PD + FoG with positive correlations, two PD + FoG with negative correlations), while PD − FoG had negative correlations (one PD − FoG with positive correlations, 13 PD − FoG with negative correlations).

Post-hoc analysis revealed that PD + FoG and PD − FoG had significant differences in connectivity between the left GP and a few clusters in the left motor cortex (see Fig. 3, panel D) within the somatosensory Brodmann areas 1, 2, 3a, 3b and 4, as shown in Fig. 4. The control group had negative correlations between the left GP and the significant clusters in the motor cortex, whereas the PD + FoG group had positive correlations. We also found that connectivity values for the PD − FoG group were between the values from the Ct and PD + FoG groups.

To validate laterality of the findings, we repeated this analysis using as seed the right GP. ANOVA analyses identified a very small cluster (43 grayordinates) in the right Brodmann area 7 postcentral with significant differences in functional connectivity among groups. However, given the reduced size of the cluster, we did not further investigate.

We also repeated this analysis using as seeds the other two ROIs with significant differences between groups (Gordon ROI 154 (default), and Gordon ROI 69 (left vestibular)). Results, however, were not significant.

Associations between functional connectivity and behavioral measures of FoG and gait

The FoG ratio during turning and foot pitch angle at heel strike during walking (representing shuffling gait) were significantly different among groups (ANOVA tests, $F = 6.2132$, $p = 0.0045$ for FoG index; and $F = 13.0294$, $p < 1e\text{-}3$ for mean foot strike angle). Post-hoc analysis revealed that the 3 groups had significant differences in the FoG ratio (Kolmogorov-Smirnov tests, Ct/PD + FoG, $p < 1e\text{-}3$; Ct/PD − FoG, $p = 0.047$; PD + FoG/PD − FoG, $p = 0.024$) and also for mean foot strike angle (Kolmogorov-Smirnov tests, Ct/PD + FoG, $p < 1e\text{-}3$; Ct/PD − FoG, $p = 2.5e\text{–}3$; PD + FoG/PD − FoG, $p = 0.028$).

The FoG ratio was significantly related with functional connectivity between the left motor cortex and left GP, as accounted by: (1) the correlation between FoG ratio and functional connectivity and (2) the successful prediction of FoG ratio using functional connectivity data. Specifically, we found a significant correlation (Spearman correlation, $R = 0.46$, $p = 2.1e\text{-}3$, as shown in Fig. 5 panel A) between the FoG index and the mean connectivity value between the left pallidus and the clusters in the left motor cortex with significant differences between PD + FoG and PD − FoG (clusters shown in Fig. 3 panel D and Fig. 4). Importantly, this correlation was not driven by differences among groups (Ct, PD + FoG and PD − FoG) as revealed by an analysis of covariance testing for differences in slopes for each group ($F = 0.48$, $p = 0.62$).

PLSR models predicting the FoG ratio using functional connectivity rendered a very large effect size (Cohen $d = 1.50$) when comparing mean absolute errors (absolute value of the difference between the predicted and observed FoG indices) for models trained with the proper FoG indices (alternative) *versus* using permuted data (null) as also shown in Fig. 5 panel A. Models were trained preserving 16 components. Strength of the results did not change when using different number of components.

Repeating the two analyses using the connectivity between left GP and the larger cluster in the motor- cortex with significant differences among the 3 groups (i.e., Fig. 3 panel A) also showed significant associations between functional connectivity and the FoG index (correlations, $R = 0.45$, $p = 2.4e\text{-}3$, and very large effect size ($d = 1.98$)).

The foot pitch angle at heel strike, representing shuffling of gait, was also significantly related to changes in functional connectivity between the left GP and motor cortex. Specifically, foot angle showed a negative correlation with mean connectivity ($R = -0.53$, $p = 4e\text{-}4$ with no evidence of differences in slopes among groups, no covariance, $F = 0.75$, $p = 0.48$) and large effect size (Cohen $d = 1.15$) and connectivity predicted mean strike foot angle compared to null hypothesis data (via permutations), as shown in Fig. 5 panel B. In fact, all the motor-cortex areas with significant differences among the three groups (Ct, PD + FoG, and PD − FoG, as shown in Fig. 3, Panel D) exhibited similar relationships between foot angle and connectivity ($R = -0.50$, $p = 8e\text{-}4$ for correlations and very large effect size ($d = 1.79$) for predictions).

While our sample was matched for disease severity based on the MDS-UPDRS Part III (Table 1), there were differences in disease duration ($p = 0.03$) with PD + FoG mean disease duration of 8.88 years and PD − FoG disease duration of 4.49 years. We found, however, no

significant correlation between functional connectivity and disease duration (Spearman correlation coefficient $R = 0.27$, $p = 0.17$) and a small effect size when predicting disease duration (Cohen $d = 0.45$, Fig. 5 panel C).

DISCUSSION

Results of this study support our hypothesis as FoG in people with PD is associated with abnormal connectivity between the left GP and the left somatosensory cortex as well as between regions belonging to the default mode network and the insular/vestibular network. Differences in functional connectivity were assessed at two different spatial resolutions: functional networks and whole brain connectivity from particular seeds. Results showed significant differences in functional connectivity between Ct and people with PD in sensorimotor, subcortical, visual and higher order heteromodal systems (Dorsal Attention, Cingular-Opercular, Default). Seed-based analysis revealed significant differences in functional connectivity between PD − FoG and PD + FoG for the left GP and two ROIs in the left somatosensory cortex and between two ROIs belonging to the default mode network and the insular/vestibular system. For both the left GP-left somatosensory cortex and for the default-vestibular areas, we found significant correlations between functional connectivity and objective measures of FoG. In this study, importantly, we used high quality data, matched samples on age, disease severity, cognitive status or levodopa medication, validated differences in connectivity with data from sensors and obtained similar results after repeating analyses using data of different quality, suggesting findings are indeed generalizable.

Functional connectivity's signature of PD includes not only motor but also higher order attention systems

Consistent with previous studies, we found that PD is associated with changes in brain functional connectivity that not only includes motor and subcortical nuclei, but also default, visual and attention systems (Fling et al., 2014; Canu et al., 2015; Fasano et al., 2015; Gilat et al., 2017, 2018; Gratton et al., 2018; Strafella et al., 2018). It has been hypothesized that these heteromodal systems are involved in execution of automatic, habitual movements affected by PD (Gilat et al, 2017). Lack of motor automaticity is common in PD, as manifested by reduced or impaired performance of learned behaviors, such as walking (Wu and Hallett, 2005; Wu et al., 2015; Bannard et al., 2019). People with PD who have FoG show less automatic walking and turning, as suggested by larger dual-task cost, more variable stride time, and larger activation of prefrontal areas (Klucken et al., 2015; Maidan et al., 2015; Mancini et al., 2018; Stuart and Mancini, 2019). A putative strategy to compensate for lack of automaticity is to rely more on attentional resources and studies have showed increases in pre-frontal cortical brain activity during movements that should be controlled automatically in PD, especially in those with FoG, compared to control subjects (Morris et al., 1996; Wu et al., 2015; Stuart and Mancini, 2019).

Importantly, our results were obtained using all the connectivity values after grouping them by functional network pair. This approach, opposed to averaging connectivity values,

considers potential heterogeneity among networks and also corrects for inflated covariance resulting from repeated measurements from the same individuals.

FoG is associated with abnormal functional connectivity between the left GP and left somatosensory cortex

We found significant differences in functional connectivity between the left GP and specific ROIs in the somatosensory cortex for Ct, PD + FoG and PD − FoG (Figs. 2–4). Specifically, mean connectivity between left GP and the left somatosensory cortex was larger in people with PD than Ct, and it was positive for PD + FoG but negative for PD − FoG. In fact, our results suggest that functional connectivity between the left GP and the somatosensory cortex could be a good predictor of FoG since most of the participants with FoG had positive functional connectivity. Furthermore, all the participants also exhibited very significant correlations between these brain areas and the FoG index. That is, the stronger the connectivity between the GP and sensorimotor cortex, the more severe the trembling of the knees associated with FoG while turning 360 degrees.

It is not surprising that abnormal connectivity between the GP and sensorimotor cortex is associated with FoG. The GP, a key output nucleus of the basal ganglia, plays a significant role in modulating the force of movements and pallidal activity is larger and more synchronized in PD than in age-matched control subjects (Oswal et al., 2013; Wilson, 2013; Feingold et al., 2015). Human recordings (Brown et al., 2001) as well as animal models of (Mallet et al., 2008; Connolly et al., 2015) have shown that such activity becomes more organized in PD with bursts of coherent oscillations in the beta band for cells in the pallidus (Bar-Gad et al., 2003; Wilson, 2013) and beta activity has been associated with FoG (Toledo et al., 2014; Anidi et al., 2018). Functional MRI detects changes in beta band activity (Parkes et al., 2006; Formaggio et al., 2008). However, our imaging cannot differentiate between activity of the internus, *versus* externus, GP, affecting the direct, and indirect, pathways, respectively. Nevertheless, the effect of PD on increased inhibitory output of the basal ganglia on the motor thalamus, results in decreased thalamocortical outputs and bradykinesia (Bergman et al., 1990; DeLong and Wichmann, 2007). It is likely that the smaller pitch of the foot at heel strike in the PD + FoG, compared to the PD − FoG, reflects shuffling gait associated with bradykinesia.

The importance of the GP in FoG is supported by studies showing that insults to the GP can result in FoG. FoG is sometimes an unintended consequence of deep brain stimulation when the electrodes are located in the GP (Schrader et al., 2011; Baizabal-Carvallo and Jankovic, 2016). Hypoxic lesions constrained to the GP can develop FoG (as well as speech disorders, axial bradykinesia and postural disturbances) but no rigidity, tremor, and almost no distal akinesia (Fève et al., 1993; Krystkowiak et al., 2006). Bilateral pallidotomy has also been associated with FoG (Merello et al., 2001). It is important to note, however, that lesions to other sites can also lead to FoG (Nutt et al., 2011; Fasano et al., 2017), including the amygdala, putamen, caudate, PPN, SMA, subthalamic nucleus (Kuo et al., 2008; Shine et al., 2013a; Fling et al., 2014; Vercruysse et al., 2014; Canu et al., 2015; Fasano et al., 2015; Gilat et al., 2017, 2018).

Interestingly, we found that differences in functional connectivity between the left GP (but not the right GP) and the left (but not the right) sensorimotor cortex was associated with FoG. This pallidal laterality may be explained by the higher concentration of dopamine and choline acetyltransferase found in the left, compared to right GP, as characterized postmortem (Glick et al., 1982). Thus, the left pallidus may be more susceptible to the reduced availability of these neurotransmitters in PD. Interestingly, reduction in both the dopaminergic and cholinergic systems have been associated with FoG (Fasano et al., 2015; Bohnen et al., 2019). The increased functional connectivity between the left GP and the left sensorimotor cortex in freezers may be to compensate for the reduced neurotransmitters. We previously demonstrated increased laterality of functional connectivity between the PPN and SMA ROIs in freezers, compared to nonfreezers as a compensation for reduced structural connectivity in these pathways (Fling et al., 2013).

Since the left GP is involved in processing left cortical activity, FoG may be related to impaired cortical control of gait from the left cortical areas. Since all of our PD subjects were right-handed, the left, dominant hemisphere may be more critical for avoiding FoG than the non-dominant hemisphere. The dominant motor cortex is specialized for intentional, precision reaching, such as step initiation or foot placement on targets, whereas the non-dominant motor cortex is specialized for postural holding, such as occurs in stance and in the single support phase of gait (Sainburg, 2014).

FoG is also associated with negative functional connectivity in the default and vestibular networks

PD participants had reduced functional connectivity compared to controls and the PD + FoG had even more negative connectivity compared to PD − FoG between the default and vestibular networks. The vestibular ROI (Guldin and Grüsser, 1998) includes the retroinsular cortex (area RI) and the lateral Belt area in the early auditory cortex, as defined by the parcellation schema derived from the Human Connectome Project (Glasser et al., 2016). Among their relevant connections are the sensory Brodmann areas 1, 2, 3a, and 3b and the motor area 4, superior premotor frontal eye field area (FEF), Brodmann area 6 m (posterior), and inferior premotor area 6v as well as to other visual and insulo-opercular brain areas (Baker et al., 2018b). In fact, the vestibular cortex is really a multisensory integration area with inputs from somatosensory, visual and vestibular inputs, all critical for postural control (MacKinnon, 2018). The default ROI covers partially the Brodmann areas 8A (dorsal) and 46 (Glasser et al., 2016) and is involved in goal-oriented attention and in the orientation to auditory and visual cues (Baker et al., 2018a), which are also part of attentional systems (Corbetta and Shulman, 2002; Vossel et al., 2014). This abnormal connectivity between the attention and default networks in PD + FoG may be consistent with the enhanced value of external auditory or visual cues that may direct attention on stepping given their loss of internal, automatic control of gait (Ginis et al., 2018). Our findings highlight the importance of multisensory integration and attention in FoG.

Functional connectivity is associated with objective measures of FoG and gait

One of the problems in studying FoG is difficulty measuring severity of freezing since FoG episodes occur sporadically in daily life but inconsistently in the clinic or research facility.

Freezing status is typically assigned by self-reports, but this is not reliable as participants don't always correctly identify their gait difficulties with FoG (Nieuwboer et al., 2009). Recently, an objective measure of freezing severity has been developed using inertial sensor measures from the lower legs (Mancini et al., 2019). This index of FoG uses a ratio of high to low frequencies of leg motion to quantify the relative amount of nonproductive trembling of the knees compared to functional gait motions (Okuma, 2006; Moore et al., 2008). Since turning in place is a reliable method to reveal FoG, we calculated the FoG ratio during repetitive 360 degree turns. We also quantified foot angle at heel strike as a measure of shuffling of gait, characteristic of PD, especially those with FoG.

The PD + FoG group in our study showed significantly worse objective FoG index and smaller foot strike angle compared to PD − FoG. Furthermore, regardless of freezing status (i.e., group assignment), the FoG index and the foot strike angle values were associated with increased functional connectivity between the left GP and the somatosensory cortex as accounted by (a) the correlation coefficient between each outcome and mean functional connectivity, and (b) the ability to predict gait outcomes based on imaging. Importantly, such predictions were assessed using hold-out cross validation and contrasted against null-hypothesis data obtained via permutations. This robust approach to estimate associations between imaging and non-imaging data suggest that altered functional connectivity has a direct effect on severity of freezing while turning as well as on shuffling of gait during straight walking.

Findings are not driven by disease duration

While not every person affected by PD will develop FoG, the likelihood of developing this condition increases with disease duration and severity. We were able to match participants based on disease severity (as well as for age, MoCA and medication, as shown in Table 1) but not on disease duration. The low and non-significant correlation between functional connectivity (pallido-motor) and disease duration (Spearman correlation $R = 0.27$, $p = 0.17$) and the low predictability of disease duration based on neuroimaging suggest that our findings are not driven by disease duration.

All the steps we followed might suggest that our findings are unlikely to be driven by other relevant factors such as registration of brain areas across participants, age, disease severity, disease duration, cognitive status or levodopa medication.

Limitations

One of the challenges when characterizing differences in functional connectivity in FoG is that there are several clinical variables that might lead to conflicting findings. Here we decided to use the highest quality imaging data from participants after matching groups on disease severity, MoCA scores, LED medication and age, ending up with a sample of moderate size ($n = 43$). While our sample was reduced, we aimed to make sure all included data met the highest quality standards and to minimize the risk our findings could be driven by uncontrolled variables. Our main result, importantly, persists even when using unmatched data ($n = 75$) and/ or less stringent head motion censoring cutoffs ($n = 81$), suggesting robustness of our findings. Another limitation of this study is the difference in disease

duration for PD + FoG and PD − FoG. Given the nature of FoG, most of the participants affected by this sign have had the disease for more time. However, the lack of association between disease duration and functional connectivity suggest our results are not driven by this clinical variable.

Another limitation is that we did not have individual ROIs for the internal and external sections of the GP because we used the default 19 subcortical ROIs as defined by FreeSurfer. Clinical cases, however, have shown that lesions to the GP (internal and external) lead to FoG (Fève et al., 1993; Merello et al., 2001; Krystkowiak et al., 2006). Future studies might be required to assess the specificity of the GPi and GPe on FoG. Similarly, the activity of the cerebellum in FreeSurfer is reported only by hemisphere, i.e., we only used two ROIs, one for the left and another for the right cerebellum. Any potential differences within the cerebellum might have been diluted by the average activity. Parcellating the cerebellum into several functional ROIs might reveal involvement of this important brain area in FoG.

In this study, we showed that FoG is associated with significant differences in functional connectivity between (a) the left GP and the left somatosensory cortex and (b) two brain areas located in the left default mode network and the left vestibular/retroinsular cortex. This lateralized differences in connectivity are also associated with objective metrics of freezing and shuffling of gait. While FOG might be multifactorial and elusive, this study suggests that impaired lateralized connectivity from the left GP is a robust feature in FOG. Our findings highlight the importance of lateralized motor loops and multisensory integration in the pathology of FoG.

Supplementary Material

Refer to Web version on PubMed Central for supplementary material.

ACKNOWLEDGMENTS

Funding: This Research was supported by the Tartar's Family Fellowship (Miranda-Dominguez), OHSU Parkinson Center of Oregon Pilot Grant GBNEU0408A (Miranda-Dominguez), National Institute on Aging (NIA) grant 5R01 AG006457, US Department of Veterans Affairs VA grant: I01 RX001075, National Institutes of Health National Institute of Mental Health (NIMH) grants R01MH115357 (Fair) and a Supplement to Promote Diversity R01MH115357-02S1 (Hermosillo).

Abbreviations:

FoG	Freezing of gait
PD	Parkinson's disease
GP	globus pallidus
SMA	supplementary motor area
PPN	pedunculopontine nuclei
ROIs	Regions of Interest

REFERENCES

Anidi C, O'Day JJ, Anderson RW, Afzal MF, Syrkin-Nikolau J, Velisar A, Bronte-Stewart HM (2018) Neuromodulation targets pathological not physiological beta bursts during gait in Parkinson's disease. Neurobiol Dis 120:107–117. [PubMed: 30196050]

Avants BB, Tustison NJ, Song G, Cook PA, Klein A, Gee JC (2011) A reproducible evaluation of ANTs similarity metric performance in brain image registration. Neuroimage 54:2033–2044. [PubMed: 20851191]

Baizabal-Carvallo JF, Jankovic J (2016) Movement disorders induced by deep brain stimulation. Parkinsonism Relat Disord 25:1–9. [PubMed: 26806438]

Baker CM, Burks JD, Briggs RG, Conner AK, Glenn CA, Morgan JP, Stafford J, Sali G, McCoy TM, Battiste JD, O'Donoghue DL, Sughrue ME (2018) A connectomic atlas of the human cerebrum-Chapter 2: The lateral frontal lobe. Oper Neurosurg (Hagerstown, Md) 15:S10–S74.

Baker CM, Burks JD, Briggs RG, Conner AK, Glenn CA, Robbins JM, Sheets JR, Sali G, McCoy TM, Battiste JD, O'Donoghue DL, Sughrue ME (2018b) A connectomic atlas of the human cerebrum: The insula and opercular cortex-Chapter 5. Oper Neurosurg (Hagerstown, Md) 15:S175–S244.

Bannard C, Leriche M, Bandmann O, Brown CH, Ferracane E, Sánchez-Ferro Á, Obeso J, Redgrave P, Stafford T (2019) Reduced habit-driven errors in Parkinson's disease. Sci Rep 9:3423. [PubMed: 30833640]

Bar-Gad I, Heimer G, Ritov Y, Bergman H (2003) Functional correlations between neighboring neurons in the primate globus pallidus are weak or nonexistent. J Neurosci 23:4012–4016. [PubMed: 12764086]

Bergman H, Wichmann T, DeLong MR (1990) Reversal of experimental parkinsonism by lesions of the subthalamic nucleus. Science 249:1436–1438. [PubMed: 2402638]

Biswal B, Yetkin FZ, Haughton VM, Hyde JS (1995) Functional connectivity in the motor cortex of resting human brain using echo-planar MRI. Magn Reson Med 34:537–541. [PubMed: 8524021]

Bohnen NI, Kanel P, Zhou Z, Koeppe RA, Frey KA, Dauer WT, Albin RL, Müller MLTMLTM (2019) Cholinergic system changes of falls and freezing of gait in Parkinson's disease. Ann Neurol.

Brown P, Oliviero A, Mazzone P, Insola A, Tonali P, Di Lazzaro V (2001) Dopamine dependency of oscillations between subthalamic nucleus and pallidum in Parkinson's disease. J Neurosci 21:1033–1038. [PubMed: 11157088]

Canu E, Agosta F, Sarasso E, Volontè MA, Basaia S, Stojkovic T, Stefanova E, Comi G, Falini A, Kostic VS, Gatti R, Filippi M (2015) Brain structural and functional connectivity in Parkinson's disease with freezing of gait. Hum Brain Mapp 36:5064–5078. [PubMed: 26359798]

Connolly AT, Jensen AL, Bello EM, Netoff TI, Baker KB, Johnson MD, Vitek JL (2015) Modulations in oscillatory frequency and coupling in globus pallidus with increasing parkinsonian severity. J Neurosci 35:6231–6240. [PubMed: 25878293]

Corbetta M, Shulman GL (2002) Control of goal-directed and stimulus-driven attention in the brain. Nat Rev Neurosci 3:201–215. [PubMed: 11994752]

Dale AM, Fischl B, Sereno MI (1999) Cortical surface-based analysis. I. Segmentation and surface reconstruction. Neuroimage 9:179–194. [PubMed: 9931268]

DCAN-Labs, 2019 DCAN-Labs/abcd-hcp-pipeline: v0.0.1: Singularity hotfix. zenodo.

DeLong MR, Wichmann T (2007) Circuits and circuit disorders of the basal ganglia. Arch Neurol 64:20–24. [PubMed: 17210805]

Desikan RS, Segonne F, Fischl B, Quinn BT, Dickerson BC, Blacker D, Buckner RL, Dale AM, Maguire RP, Hyman BT, Albert MS, Killiany RJ (2006) An automated labeling system for subdividing the human cerebral cortex on MRI scans into gyral based regions of interest. Neuroimage 31:968–980. [PubMed: 16530430]

Fair DA et al. (2013) Distinct neural signatures detected for ADHD subtypes after controlling for micro-movements in resting state functional connectivity MRI data. Front Syst Neurosci 6:80. [PubMed: 23382713]

Fair DA et al. (2020) Correction of respiratory artifacts in MRI head motion estimates. Neuroimage 208 116400. [PubMed: 31778819]

Fair DA, Cohen AL, Power JD, Dosenbach NU, Church JA, Miezin FM, Schlaggar BL, Petersen SE (2009) Functional brain networks develop from a “local to distributed” organization. PLoS Comput Biol 5 e1000381. [PubMed: 19412534]

Fair DA, Schlaggar BL, Cohen AL, Miezin FM, Dosenbach NUF, Wenger KK, Fox MD, Snyder AZ, Raichle ME, Petersen SE (2007) A method for using blocked and event-related fMRI data to study “resting state” functional connectivity. Neuroimage 35:396–405. [PubMed: 17239622]

Fasano A, Herman T, Tessitore A, Strafella AP, Bohnen NI (2015) Neuroimaging of Freezing of Gait. J Parkinsons Dis 5:241–254. [PubMed: 25757831]

Fasano A, Laganiere SE, Lam S, Fox MD (2017) Lesions causing freezing of gait localize to a cerebellar functional network. Ann Neurol 81:129–141. [PubMed: 28009063]

Feingold J, Gibson DJ, DePasquale B, Graybiel AM (2015) Bursts of beta oscillation differentiate postperformance activity in the striatum and motor cortex of monkeys performing movement tasks. Proc Natl Acad Sci U S A 112:13687–13692. [PubMed: 26460033]

Fève AP, Fénelon G, Wallays C, Rémy P, Guillard A (1993) Axial motor disturbances after hypoxic lesions of the globus pallidus. Mov Disord 8:321–326. [PubMed: 8341296]

Fischl B et al. (2002) Whole brain segmentation: automated labeling of neuroanatomical structures in the human brain. Neuron 33:341–355. [PubMed: 11832223]

Fischl B, Dale AM (2000) Measuring the thickness of the human cerebral cortex from magnetic resonance images. Proc Natl Acad Sci U S A 97:11050–11055. [PubMed: 10984517]

Fischl B, Salat DH, van der Kouwe AJ, Makris N, Segonne F, Quinn BT, Dale AM (2004) Sequence-independent segmentation of magnetic resonance images. Neuroimage 23(Suppl 1):S69–S84. [PubMed: 15501102]

Fling BW, Cohen RG, Mancini M, Carpenter SD, Fair DA, Nutt JG, Horak FB (2014) Functional reorganization of the locomotor network in Parkinson patients with freezing of gait. PLoS One 9 e100291. [PubMed: 24937008]

Fling BW, Cohen RG, Mancini M, Nutt JG, Fair DA, Horak FB (2013) Asymmetric pedunculopontine network connectivity in parkinsonian patients with freezing of gait. Brain 136:2405–2418. [PubMed: 23824487]

Formaggio E, Storti SF, Avesani M, Cerini R, Milanese F, Gasparini A, Acler M, Pozzi Mucelli R, Fiaschi A, Manganotti P (2008) EEG and FMRI coregistration to investigate the cortical oscillatory activities during finger movement. Brain Topogr 21:100–111. [PubMed: 18648924]

Fox MD, Raichle ME (2007) Spontaneous fluctuations in brain activity observed with functional magnetic resonance imaging. Nat Rev Neurosci 8:700–711. [PubMed: 17704812]

Friston KJ, Mechelli A, Turner R, Price CJ (2000) Nonlinear responses in fMRI: the Balloon model, Volterra kernels, and other hemodynamics. Neuroimage 12:466–477. [PubMed: 10988040]

Gibb WR, Lees AJ (1989) The significance of the Lewy body in the diagnosis of idiopathic Parkinson’s disease. Neuropathol Appl Neurobiol 15:27–44. [PubMed: 2542825]

Gilat M, Bell PT, Ehgoetz Martens KA, Georgiades MJ, Hall JM, Walton CC, Lewis SJG, Shine JM (2017) Dopamine depletion impairs gait automaticity by altering cortico-striatal and cerebellar processing in Parkinson’s disease. Neuroimage 152:207–220. [PubMed: 28263926]

Gilat M, Ehgoetz Martens KA, Miranda-Domínguez O, Arpan I, Shine JM, Mancini M, Fair DA, Lewis SJGG, Horak FB (2018) Dysfunctional limbic circuitry underlying freezing of gait in Parkinson’s disease. Neuroscience 374:119–132. [PubMed: 29408498]

Ginis P, Nackaerts E, Nieuwboer A, Heremans E (2018) Cueing for people with Parkinson’s disease with freezing of gait: A narrative review of the state-of-the-art and novel perspectives. Ann Phys Rehabil Med 61:407–413. [PubMed: 28890341]

Glasser MF, Coalson TS, Robinson EC, Hacker CD, Harwell J, Yacoub E, Ugurbil K, Andersson J, Beckmann CF, Jenkinson M, Smith SM, Van Essen DC (2016) A multi-modal parcellation of human cerebral cortex. Nature 536:171–178. [PubMed: 27437579]

Glasser MF, Sotiropoulos SN, Wilson JA, Coalson TS, Fischl B, Andersson JL, Xu J, Jbabdi S, Webster M, Polimeni JR, Van Essen DC, Jenkinson M (2013) The minimal preprocessing pipelines for the Human Connectome Project. Neuroimage 80:105–124. [PubMed: 23668970]

Glick SD, Ross DA, Hough LB (1982) Lateral asymmetry of neurotransmitters in human brain. Brain Res 234:53–63. [PubMed: 6120746]

Goetz CG et al. (2008) Movement Disorder Society-sponsored revision of the Unified Parkinson's Disease Rating Scale (MDS-UPDRS): scale presentation and clinimetric testing results. Mov Disord 23:2129–2170. [PubMed: 19025984]

Gordon EM, Laumann TO, Adeyemo B, Huckins JF, Kelley WM, Petersen SE (2014) Generation and evaluation of a cortical area parcellation from resting-state correlations. Cereb Cortex 26:288–303. [PubMed: 25316338]

Gratton C, Koller JM, Shannon W, Greene DJ, Snyder AZ, Petersen SE, Perlmutter JS, Campbell MC, Greene J, Snyder AZ, Petersen SE, Perlmutter JS, Campbell MC (2018) Emergent functional network effects in Parkinson disease. Cereb Cortex:1–15. [PubMed: 29253248]

Grayson DS, Fair DA (2017) Development of large-scale functional networks from birth to adulthood: a guide to the neuroimaging literature. Neuroimage 160:15–31. [PubMed: 28161313]

Guldin WO, Grüsser OJ (1998) Is there a vestibular cortex? Trends Neurosci 21:254–259. [PubMed: 9641538]

Holodny AI (2009) Functional neuroimaging: A clinical approach. Am J Neuroradiol 30:e61–e62.

Jankovic J (2008) Parkinson's disease: clinical features and diagnosis. J Neurol Neurosurg Psychiatry 79:368–376. [PubMed: 18344392]

Jenkinson M, Beckmann CF, Behrens TEJ, Woolrich MW, Smith SM (2012). FSL. Neuroimage 62:782–790. [PubMed: 21979382]

Kasper (2015) Harrison's principles of internal medicine. McGraw-Hill.

Klucken J, Friedl KE, Eskofier BM, Hausdorf JM (2015) Guest Editorial: enabling technologies for Parkinson's disease management. IEEE J Biomed Heal Informatics 19:1775–1776.

Kovacs-Balint Z, Feczko E, Pincus M, Earl E, Miranda-Dominguez O, Howell B, Morin E, Maltbie E, Li L, Steele J, Styner M, Bachevalier J, Fair D, Sanchez M (2019) Early developmental trajectories of functional connectivity along the visual pathways in rhesus monkeys. Cereb Cortex 29:3514–3526. [PubMed: 30272135]

Krystkowiak P, Delval A, Dujardin K, Bleuse S, Blatt JL, Bourriez JL, Derambure P, Destée A, Defebvre L (2006) Gait abnormalities induced by acquired bilateral pallidal lesions: a motion analysis study. J Neurol 253:594–600. [PubMed: 16525880]

Kuo S-H, Kenney C, Jankovic J (2008) Bilateral pedunculopontine nuclei strokes presenting as freezing of gait. Mov Disord 23:616–619. [PubMed: 18181207]

Lenka A, Naduthota RM, Jha M, Panda R, Prajapati A, Jhunjhunwala K, Saini J, Yadav R, Bharath RD, Pal PK (2016) Freezing of gait in Parkinson's disease is associated with altered functional brain connectivity. Park Relat Disord 24:100–106.

MacKinnon CD (2018) Sensorimotor anatomy of gait, balance, and falls. Handb Clin Neurol 159:3–26. [PubMed: 30482322]

Maidan I, Bernad-Elazari H, Gazit E, Giladi N, Hausdorff JM, Mirelman A (2015) Changes in oxygenated hemoglobin link freezing of gait to frontal activation in patients with Parkinson disease: an fNIRS study of transient motor-cognitive failures. J Neurol 262:899–908. [PubMed: 25636682]

Maidan I, Jacob Y, Giladi N, Hausdorff JM, Mirelman A (2019) Altered organization of the dorsal attention network is associated with freezing of gait in Parkinson's disease. Parkinsonism Relat Disord.

Mallet N, Pogosyan A, Márton LF, Bolam JP, Brown P, Magill PJ (2008) Parkinsonian beta oscillations in the external globus pallidus and their relationship with subthalamic nucleus activity. J Neurosci 28:14245–14258. [PubMed: 19109506]

Mancini M, Bloem BR, Horak FB, Lewis SJG, Nieuwboer A, Nonnekes J (2019) Clinical and methodological challenges for assessing freezing of gait: future perspectives. Mov Disord.

Mancini M, Curtze C, Stuart S, El-Gohary M, James McNames, Nutt JG, Horak FB (2018) The impact of freezing of gait on balance perception and mobility in community-living with Parkinson's disease. In: 2018 40th annual international conference of the IEEE engineering in medicine and biology society (EMBC) IEEE p. 3040–3043.

Mancini M, Smulders K, Cohen RG, Horak FB, Giladi N, Nutt JG (2017) The clinical significance of freezing while turning in Parkinson's disease. Neuroscience 343:222–228. [PubMed: 27956066]

Marcus DS, Harwell J, Olsen T, Hodge M, Glasser MF, Prior F, Jenkinson M, Laumann T, Curtiss SW, Van Essen DC (2011) Informatics and data mining tools and strategies for the Human Connectome Project. Front Neuroinform:5.

Merello M, Starkstein S, Nouzeilles MI, Kuzis G, Leiguarda R (2001) Bilateral pallidotomy for treatment of Parkinson's disease induced corticobulbar syndrome and psychic akinesia avoidable by globus pallidus lesion combined with contralateral stimulation. J Neurol Neurosurg Psychiatry 71:611–614. [PubMed: 11606671]

Mills BD, Miranda-Dominguez O, Mills KL, Earl E, Cordova M, Painter J, Karalunas SL, Nigg JT, Fair DA (2018) ADHD and attentional control: Impaired segregation of task positive and task negative brain networks. Netw Neurosci (Cambridge, Mass) 2:200–217.

Miranda-Dominguez O, Feczko E, Grayson DS, Walum H, Nigg JT, Fair DA (2018) Heritability of the human connectome: A connectotyping study. Netw Neurosci (Cambridge, Mass) 2:175–199.

Moore GA, Hill-Soderlund AL, Propper CB, Calkins SD, Mills-Koonce WR, Cox MJ (2009) Mother-infant vagal regulation in the face-to-face still-face paradigm is moderated by maternal sensitivity. Child Dev 80:209–223. [PubMed: 19236402]

Moore ST, Dilda V, Hakim B, Macdougall HG (2011) Validation of 24-hour ambulatory gait assessment in Parkinson's disease with simultaneous video observation. Bsiomed Eng Online 10:82.

Moore ST, MacDougall HG, Ondo WG (2008) Ambulatory monitoring of freezing of gait in Parkinson's disease. J Neurosci Methods 167:340–348. [PubMed: 17928063]

Morris ME, Iansek R, Matyas TA, Summers JJ (1996) Stride length regulation in Parkinson's disease. Normalization strategies and underlying mechanisms. Brain 119(Pt 2):551–568. [PubMed: 8800948]

Nasreddine ZS, Phillips NA, Bédirian V, Charbonneau S, Whitehead V, Collin I, Cummings JL, Chertkow H (2005) The Montreal Cognitive Assessment, MoCA: a brief screening tool for mild cognitive impairment. J Am Geriatr Soc 53:695–699. [PubMed: 15817019]

Nieuwboer A, Rochester L, Herman T, Vandenberghe W, Emil GE, Thomaes T, Giladi N (2009) Reliability of the new freezing of gait questionnaire: agreement between patients with Parkinson's disease and their carers. Gait Posture 30:459–463. [PubMed: 19660949]

Nonnekes J, Snijders AH, Nutt JG, Deuschl G, Giladi N, Bloem BR (2015) Freezing of gait: a practical approach to management. Lancet Neurol 14:768–778. [PubMed: 26018593]

Nutt JG, Bloem BR, Giladi N, Hallett M, Horak FB, Nieuwboer A (2011) Freezing of gait: moving forward on a mysterious clinical phenomenon. Lancet Neurol 10:734–744. [PubMed: 21777828]

Okuma Y (2006) Freezing of gait in Parkinson's disease. J Neurol (253 Suppl):VII27–VII32. [PubMed: 17131225]

Okuma Y, Silva de Lima AL, Fukae J, Bloem BR, Snijders AH (2018) A prospective study of falls in relation to freezing of gait and response fluctuations in Parkinson's disease. Parkinsonism Relat Disord 46:30–35. [PubMed: 29079421]

Oswal A, Brown P, Litvak V (2013) Synchronized neural oscillations and the pathophysiology of Parkinson's disease. Curr Opin Neurol 26:662–670. [PubMed: 24150222]

Parkes LM, Bastiaansen MCM, Norris DG (2006) Combining EEG and fMRI to investigate the post-movement beta rebound. Neuroimage 29:685–696. [PubMed: 16242346]

Power J, Mitra A, Laumann T, Snyder A, Schlaggar B, Petersen S (2013) Methods to detect, characterize, and remove motion artifact in resting state fMRI. Neuroimage.

Power JD, Barnes KA, Snyder AZ, Schlaggar BL, Petersen SE (2012) Spurious but systematic correlations in functional connectivity MRI networks arise from subject motion. Neuroimage 59:2142–2154. [PubMed: 22019881]

Rosipal R, Kr N, Krämer N, Kr N, Krämer N (2005) Overview and recent advances in partial least squares. Int Stat Optim Perspect Work Subspace, Latent Struct Featur Sel. p. 34–51.

Rosvall M, Bergstrom CT (2008) Maps of random walks on complex networks reveal community structure. Proc Natl Acad Sci U S A 105:1118–1123. [PubMed: 18216267]

Rudolph MD, Graham AM, Feczko E, Miranda-Dominguez O, Rasmussen JM, Nardos R, Entringer S, Wadhwa PD, Buss C, Fair DA (2018) Maternal IL-6 during pregnancy can be estimated from

newborn brain connectivity and predicts future working memory in offspring. Nat Neurosci 21:765–772. [PubMed: 29632361]

Rudolph MD, Miranda-Domínguez O, Cohen AO, Breiner K, Steinberg L, Bonnie RJ, Scott ES, Taylor-Thompson K, Chein J, Fettich KC, Richeson JA, Dellarco DV, Galván A, Casey BJ, Fair DA (2017) At risk of being risky: The relationship between "brain age" under emotional states and risk preference. Dev Cogn Neurosci 24:93–106. [PubMed: 28279917]

Sainburg RL (2014) Convergent models of handedness and brain lateralization. Front Psychol 5:1092. [PubMed: 25339923]

Schrader C, Capelle H-H, Kinfe TM, Blahak C, Bäzner H, Lütjens G, Dressler D, Krauss JK (2011) GPi-DBS may induce a hypokinetic gait disorder with freezing of gait in patients with dystonia. Neurology 77:483–488. [PubMed: 21775741]

Shine JM, Matar E, Ward PB, Bolitho SJ, Gilat M, Pearson M, Naismith SL, Lewis SJG (2013a) Exploring the cortical and subcortical functional magnetic resonance imaging changes associated with freezing in Parkinson's disease. Brain 136:1204–1215. [PubMed: 23485851]

Shine JM, Matar E, Ward PB, Frank MJ, Moustafa AA, Pearson M, Naismith SL, Lewis SJG (2013b) Freezing of gait in Parkinson's disease is associated with functional decoupling between the cognitive control network and the basal ganglia. Brain 136:3671–3681. [PubMed: 24142148]

Smith SM, Jenkinson M, Woolrich MW, Beckmann CF, Behrens TEJ, Johansen-Berg H, Bannister PR, De Luca M, Drobnjak I, Flitney DE, Niazy RK, Saunders J, Vickers J, Zhang Y, De Stefano N, Brady JM, Matthews PM (2004) Advances in functional and structural MR image analysis and implementation as FSL. Neuroimage 23:S208–S219. [PubMed: 15501092]

Smith SM, Nichols TE (2009) Threshold-free cluster enhancement: addressing problems of smoothing, threshold dependence and localisation in cluster inference. Neuroimage 44:83–98. [PubMed: 18501637]

Snijders AH, Takakusaki K, Debu B, Lozano AM, Krishna V, Fasano A, Aziz TZ, Papa SM, Factor SA, Hallett M (2016) Physiology of freezing of gait. Ann Neurol 80:644–659. [PubMed: 27649270]

Strafella AP, Bohnen NI, Pavese N, Vaillancourt DE, van Eimeren T, Politis M, Tessitore A, Ghadery C, Lewis S (2018) Imaging markers of progression in Parkinson's disease. Mov Disord Clin Pract.

Stuart S, Mancini M, 2019 Pre-frontal cortical activation with open and closed-loop tactile cueing when walking and turning in Parkinson disease: a pilot study.

Tessitore A, Amboni M, Esposito F, Russo A, Picillo M, Marcuccio L, Pellecchia MT, Vitale C, Cirillo M, Tedeschi G, Barone P (2012) Resting-state brain connectivity in patients with Parkinson's disease and freezing of gait. Parkinsonism Relat Disord 18:781–787. [PubMed: 22510204]

Toledo JB, López-Azcárate J, Garcia-Garcia D, Guridi J, Valencia M, Artieda J, Obeso J, Alegre M, Rodriguez-Oroz M (2014) High beta activity in the subthalamic nucleus and freezing of gait in Parkinson's disease. Neurobiol Dis 64:60–65. [PubMed: 24361601]

Tomlinson CL, Stowe R, Patel S, Rick C, Gray R, Clarke CE (2010) Systematic review of levodopa dose equivalency reporting in Parkinson's disease. Mov Disord 25:2649–2653. [PubMed: 21069833]

van Dijsseldonk K, Wang Y, van Wezel R, Bloem BR, Nonnekes J (2018) Provoking freezing of gait in clinical practice: Turning in place is more effective than stepping in place. J Parkinsons Dis 8:363–365. [PubMed: 29710736]

Vercruysse S, Spildooren J, Heremans E, Wenderoth N, Swinnen SP, Vandenberghe W, Nieuwboer A (2014) The neural correlates of upper limb motor blocks in Parkinson's disease and their relation to freezing of gait. Cereb Cortex 24:3154–3166. [PubMed: 23861319]

Vossel S, Geng JJ, Fink GR (2014) Dorsal and ventral attention systems: distinct neural circuits but collaborative roles. Neuroscientist 20:150–159. [PubMed: 23835449]

Wilson CJ (2013) Active decorrelation in the basal ganglia. Neuroscience 250:467–482. [PubMed: 23892007]

Winkler AM, Ridgway GR, Webster MA, Smith SM, Nichols TE (2014) Permutation inference for the general linear model. Neuroimage 92:381–397. [PubMed: 24530839]

Woolrich MW, Jbabdi S, Patenaude B, Chappell M, Makni S, Behrens T, Beckmann C, Jenkinson M, Smith SM (2009) Bayesian analysis of neuroimaging data in FSL. Neuroimage 45: S173–S186. [PubMed: 19059349]

Wu T, Hallett M (2005) A functional MRI study of automatic movements in patients with Parkinson's disease. Brain 128:2250–2259. [PubMed: 15958505]

Wu T, Hallett M, Chan P (2015) Motor automaticity in Parkinson's disease. Neurobiol Dis 82:226–234. [PubMed: 26102020]

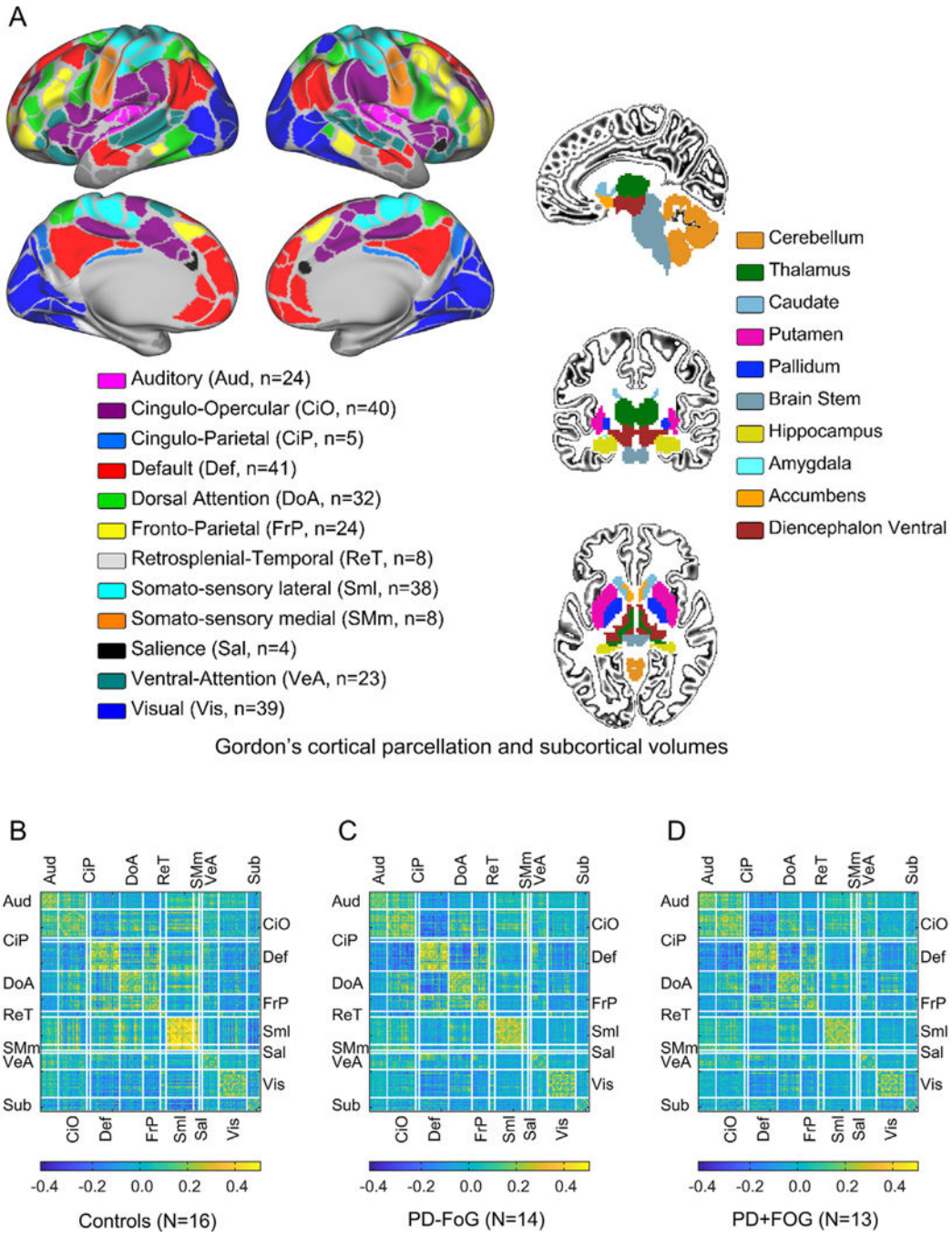

Fig. 1.

Parcellation schema and average connectivity matrices. **(A)** Gordon's parcellation schema (Gordon et al., 2014) color-coded by functional system and subcortical volumes from FreeSurfer (Fischl et al., 2002, 2004). Color-coding map also indicates the number of ROIs per network. **(B)** mean connectivity matrices for the Control (Ct) group. **(B)** PD non-freezers (PD − FoG). **(C)** PD freezers (PD + FoG). White lines indicate the borders between functional systems.

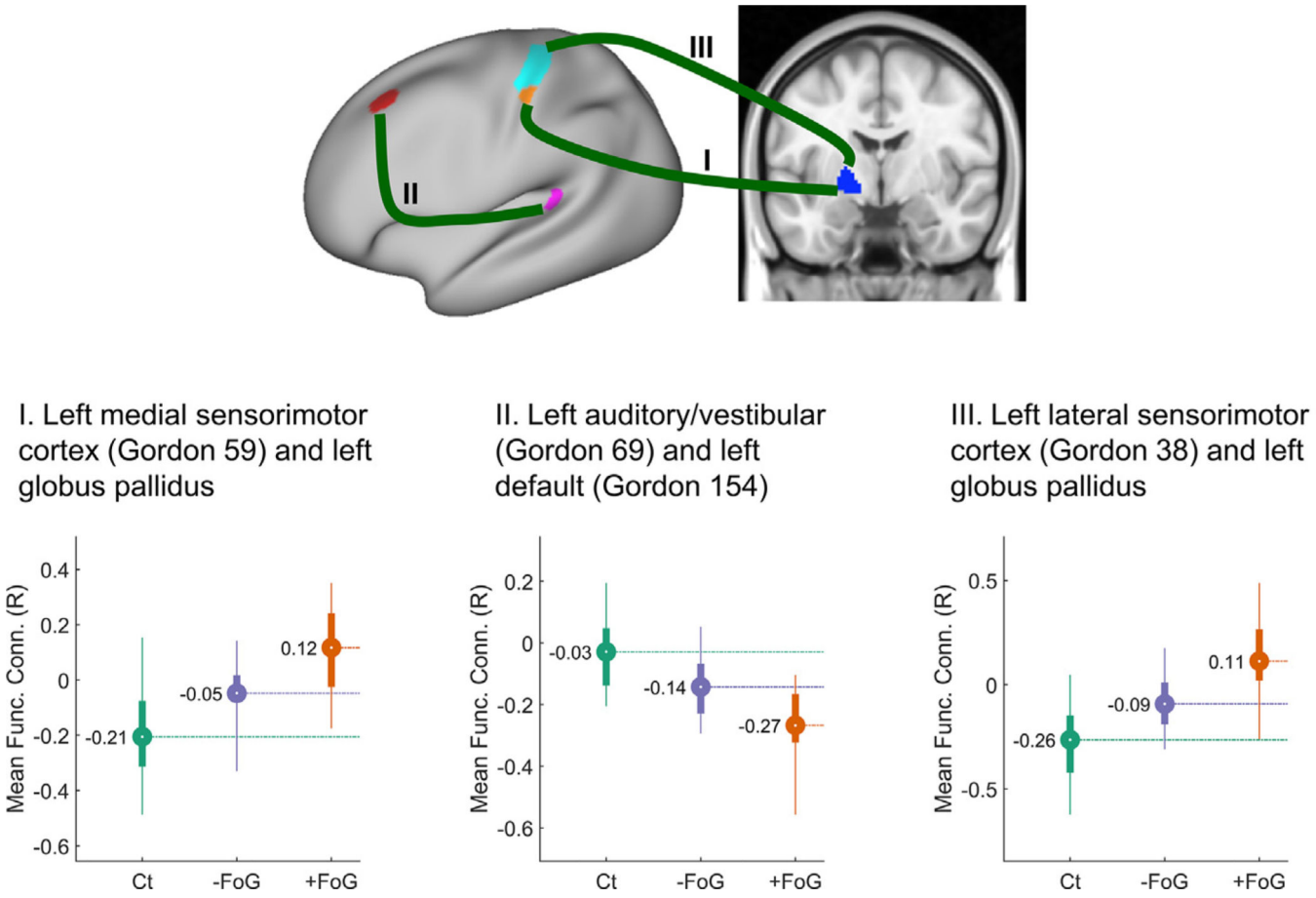

Fig. 2.

Connections with significant differences among the freezers (Ct), nonfreezers (PD − FoG) and freezers (PD + FoG) groups. *Top panel* figure shows the location of three pairs of functionally connected areas (I, II and III) with significant differences in functional connectivity among groups on a “very-inflated” map of the left cortex. *Bottom-panel* figures show the distribution of the mean functional connectivity values for each ROI pair, color-coded per diagnosis (Ct, PD + FoG, PD − FoG). Circles represent the mean functional connectivity and the bar indicates the interquartile range. Thin lines correspond to the percentiles 2.5–97.5.

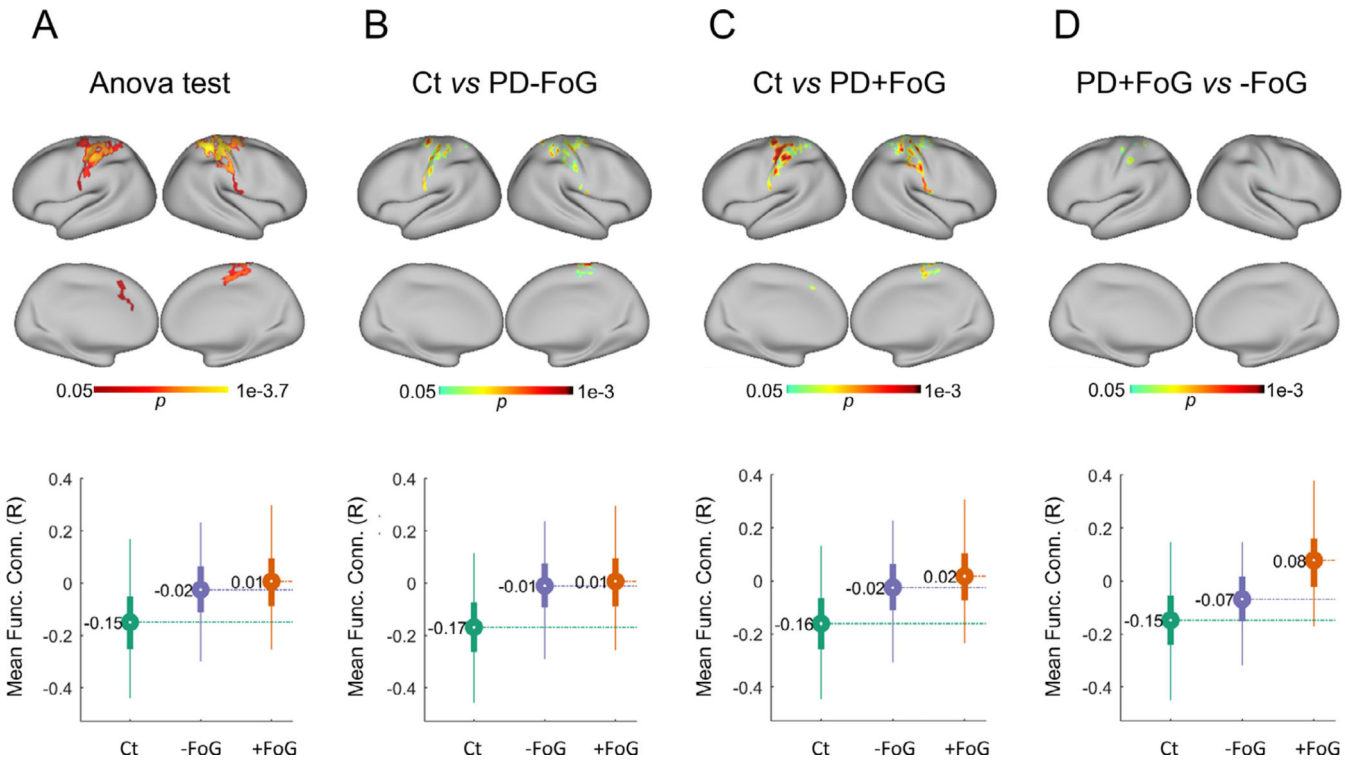

Fig. 3.

Areas with significant differences in functional connectivity from the left globus pallidus. *Top panel* figures correspond to maps of significant differences in functional connectivity among Ct, PD + FoG and PD − FoG using as seed the left globus pallidus, as revealed by an ANOVA test **(A)** and posthoc comparisons between Ct and PD − FoG **(B)**, Ct and PD + FoG **(C)**, and PD + FoG and PD − FoG **(D)**. Significant cluster in **(D)** cover partial sections of the Brodmann areas 1–4. See Fig. 4 for more details. *Bottom panel* figures show the distribution of functional connectivity between the left-pallidus and the brain areas with significant differences (circles represent the mean functional connectivity and the bar indicates the interquartile range. Thin lines correspond to the percentiles 2.5–97.5).

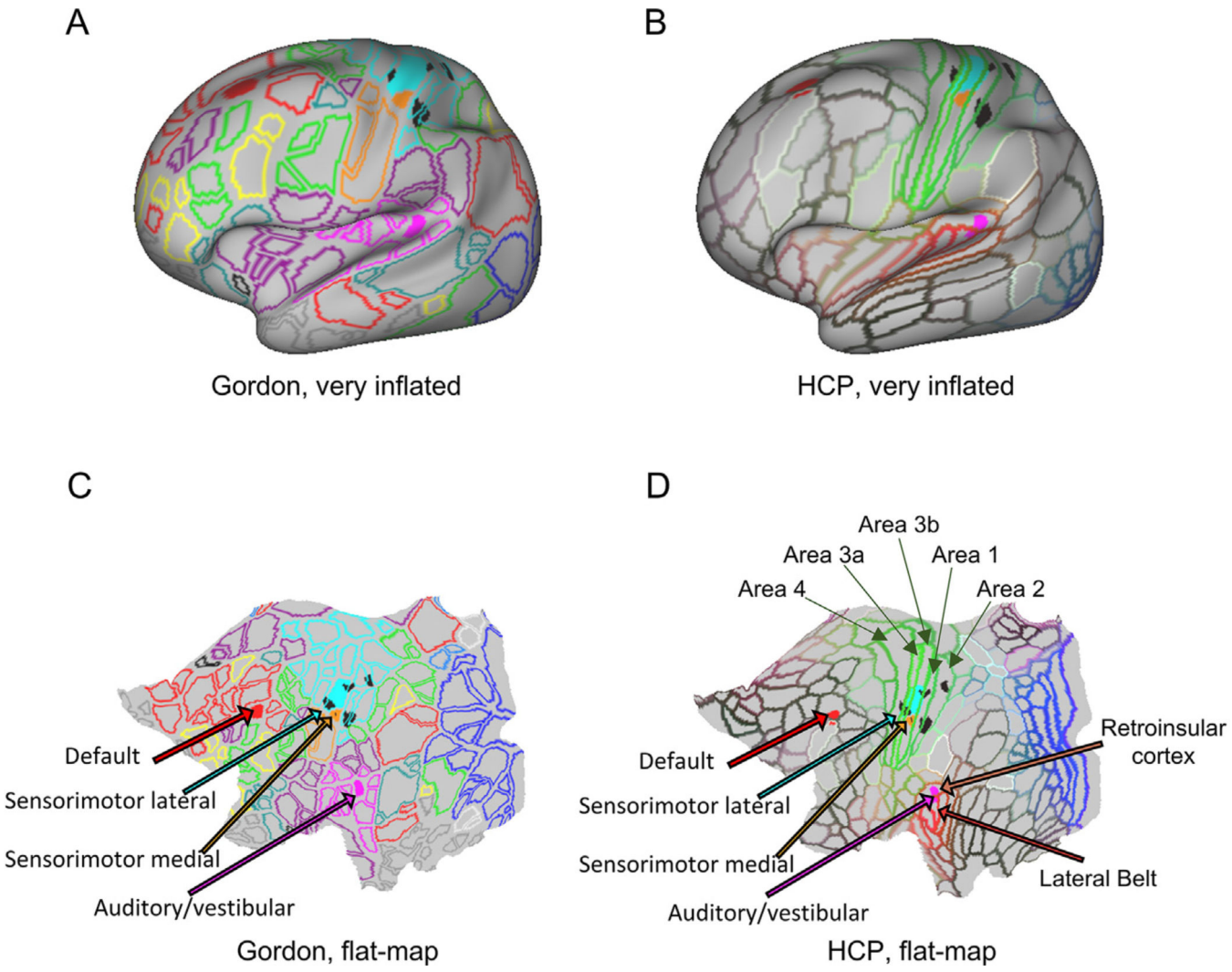

Fig. 4.

Cortical areas associated with freezing of gait. “Very inflated” and “flat map” projections of the cortical areas associated with freezing of gait on top of the delineation of regions of interest as defined by *Gordon* (Gordon et al., 2014) and the *Human Connectome Project* (HCP, (Glasser et al., 2016)). Black spots are the cortical areas in the somatosensory cortex with significant differences between PD-freezers, PD-non-freezers and controls identified by the seed analysis from the left globus pallidus (from Fig. 3(D)). Connectivity between the left globus pallidus and the areas in the sensorimotor lateral and medial cortex (Gordon ROIs 38 and 59, respectively (Gordon et al., 2014)) and between the cortical areas belonging to the Default (Gordon ROI 154) and Auditory/vestibular (Gordon 69 (Gordon et al., 2014)) networks also exhibited significant differences between groups. Legends from the HCP parcellation were included for areas overlapping the significant Gordon areas identified as relevant to FoG: Brodmann areas 1, 2, 3a, 3b, 4, 8A (dorsal), 46, lateral Belt area in the early auditory cortex and the retroinsular cortex.

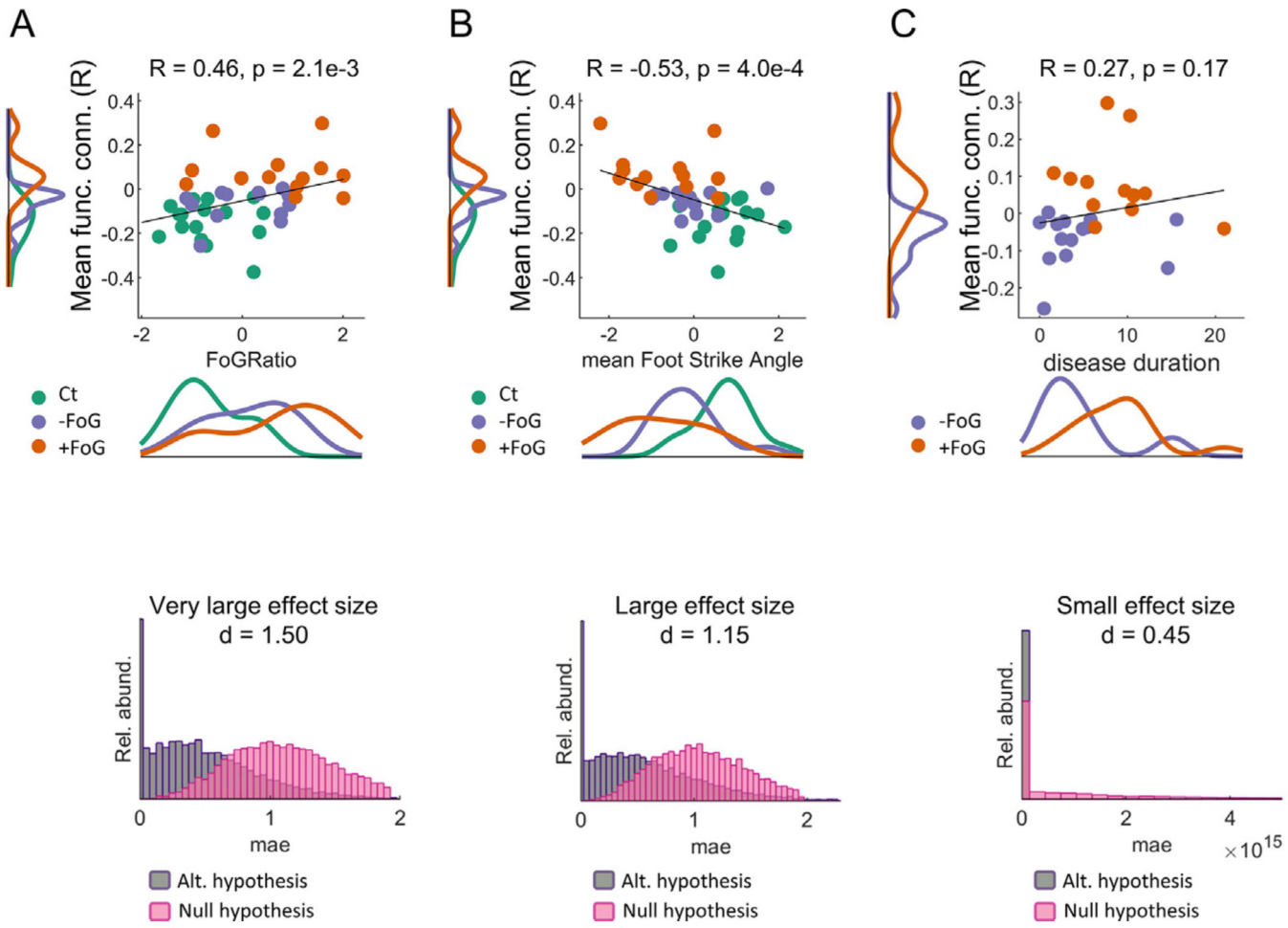

Fig. 5.

Associations between functional connectivity and FoG ratio, strike angle and disease duration. *Top panel* figures: scatter plots showing the FoG ratio **(A)**, foot strike angle **(B)**, and disease duration **(C)** *versus* mean connectivity values between the left globus pallidus and the brain clusters with significant differences between PD + FoG and PD − FoG as a function of FoG ratio, color-coded by diagnosis. *Bottom panel* figures: distribution of mean absolute errors (mae) when partial least squares models are used to predict out-of-sample values of FoG ratio, foot strike angle, and disease duration. Cohen effect size is also indicated. Notice the low association between imaging and disease duration **(C)** as accounted by the low correlation and the low accuracy of the models predicting disease duration where the mean absolute errors are of the order of 4e15 years.

Table 1.

Sample description

Characteristics	Group			*p*-values +FoG *vs*−FoG
	Control (Ct)	PD Non-Freezers (PD − FoG)	PD Freezers (PD + FoG)	
Original sample (*N* = 111)	40	42	29	
Frame displacement th = 0.5 mm, all (*N* = 103)	39	36	28	
Age	69.5 (7.71)	69.2 (7.22)	68.9 (7.39)	0.89
MDS-UPDRS III total		36.5 (11.39)	45.9 (14.89)	0.01
Duration of disease (yr)		5.9 (5.05)	9.4 (6.58)	0.02
MoCA	26.9 (1.99)	25.2 (3.48)	25.1 (4.10)	0.91
LED medication		683.9 (436.63)	1404.6 (2189.11)	0.07
Frame displacement th = 0.5 mm, matched (*N* = 81)	27	27	27	
Age	69.4 (6.35)	69.6 (7.87)	68.6 (7.50)	0.63
MDS-UPDRS III total		39.6 (12.97)	47.0 (15.77)	0.07
Duration of disease (yr)		6.8 (4.55)	9.8 (6.81)	0.06
MoCA	26.8 (2.28)	24.7 (4.11)	25.7 (4.02)	0.34
LED medication		735.1 (452.43)	1374.6 (2106.00)	0.13
Frame displacement th = 0.3 mm, all (*N* = 75)	27	27	21	
Age	68.6 (8.15)	69.0 (7.42)	69.3 (6.17)	0.90
MDS-UPDRS III total		35.0 (11.28)	43.9 (13.42)	0.02
Duration of disease (yr)		5.6 (4.44)	7.8 (5.55)	0.13
MoCA	27.0 (1.77)	24.8 (3.64)	25.5 (4.18)	0.53
LED medication		667.9 (481.05)	1525.3 (2437.50)	0.08
Frame displacement th = 0.3 mm, matched (*N* = 43)	16 (4/12)	14 (4/10)	13 (4/9)	
Age (years)	70.3 (7.3)	68.0 (7.8)	67.5 (6.0)	0.86
MDS-UPDRS III total	NA	37.6 (9.0)	40.4 (13.0)	0.53
Duration of disease (yr)	NA	4.49 (4.8)	8.88 (4.8)	0.03
MoCA	27.1 (1.9)	24.0 (3.4)	25.9 (3.4)	0.16
LED medication		573 (357.1)	594 (364.7)	0.12

Sample size reported in “count”. Number in parenthesis indicates male/female count. Mean (standard deviation) reported for the other variables. MDS-UPDRS: Movement Disorders Society Unified Parkinson’s Disease Rating Scale. MoCA: Montreal Cognitive Assessment. LEDD: Levodopa equivalent daily dosage. yr: years.